International Journal for Parasitology: Drugs and Drug Resistance 17 (2021) 139–149

Contents lists available at ScienceDirect

International Journal for Parasitology: Drugs and Drug Resistance

journal homepage: www.elsevier.com/locate/ijpddr

The therapeutic potential of novel isobenzofuranones against *Naegleria fowleri*

Aitor Rizo-Liendo [a,b,c,1], Iñigo Arberas-Jiménez [a,b,c,1], Ines Sifaoui [a,b,c,e], Dimitra Gkolfi [d], Yiset Santana [d], Leandro Cotos [d], David Tejedor [d,**], Fernando García-Tellado [d,***], José E. Piñero [a,b,c,e,****], Jacob Lorenzo-Morales [a,b,c,e,*]

[a] *Instituto Universitario de Enfermedades Tropicales y Salud Pública de Canarias, Universidad de La Laguna, Avda. Astrofísico Fco. Sánchez, S/N, La Laguna, Tenerife, 38203, Islas Canarias, Spain*

[b] *Departamento de Obstetricia, Ginecología, Pediatría, Medicina Preventiva y Salud Pública, Toxicología, Medicina Legal y Forense y Parasitología, Universidad De La Laguna, La Laguna, Tenerife, 38203, Islas Canarias, Spain*

[c] *Red de Investigación Colaborativa en Enfermedades Tropicales (RICET), Spain*

[d] *Instituto de Productos Naturales y Agrobiología, Consejo Superior de Investigaciones Científicas, Avda. Fco. Sánchez 3, 38206, La Laguna, Tenerife, Islas Canarias, Spain*

[e] *Consorcio Centro De Investigacion Biomedica En Red M.P. (CIBER) de Enfermedades Infecciosas, Inst. de Salud Carlos III, Madrid, Spain*

ARTICLE INFO

Keywords:
Naegleria
Therapeutics
Isobenzofuranones
Programmed cell death
Encephalitis

ABSTRACT

The Free-Living Amoeba species, *Naegleria fowleri* is the causative agent of a lethal encephalitis known as Primary Amoebic Encephalitis (PAM). Moreover, most of the reported cases are often related to swimming and/or diving in aquatic environments. In addition, the current therapeutic options against PAM are not fully effective and hence, there is an urgent need to develop novel therapeutic agents against this disease. Previously isobenzofuranones compounds have been reported to present antiprotozoal and antifungal activity among others. However, to the best of our knowledge, these molecules have not been previously tested against *N. fowleri*. Therefore, the aim of this study was to evaluate the activity of 14 novel isobenzofuranones against this pathogenic amoeba. The most active and less toxic molecules, were assayed in order to check induction of Programmed Cell Death (PCD) in the treated amoebae. The obtained results showed that these molecules were able to eliminate *N. fowleri* trophozoites and also induced PCD. Therefore, the tested isobenzofuranones could be potential therapeutic candidates for the treatment of PAM.

1. Introduction

The opportunistic pathogenic amoeba *Naegleria fowleri*, belonging to the Free-Living Amoeba (FLA) group, causes a fatal disease in humans known as Primary Amoebic Meningoencephalitis (PAM)(Maciver et al., 2020; Piñero et al., 2019; Visvesvara et al., 2007). Popularly known as 'brain-eating amoeba', the first PAM case was reported in Australia by Fowler and Carter in 1965 (Fowler and Carter, 1965). Since then, there has been a progressive increase in the reported cases worldwide (Maciver et al., 2020). With more than 430 cases officially reported (Bellini et al., 2018; Maciver et al., 2020; Piñero et al., 2019), the United States of America (USA) and Pakistan are the most affected countries (Debnath et al., 2020; Johnson et al., 2016; Yoder et al., 2010). Recently other countries including Brazil, Costa Rica, Philippines or India have reported new cases of PAM (Ali et al., 2020; Graciaa et al., 2018a; Henker et al., 2019; Milanez et al., 2017; Mittal et al., 2019), and at the

* Corresponding author. Instituto Universitario de Enfermedades Tropicales y Salud Pública de Canarias, Universidad de La Laguna, Avda. Astrofísico Fco. Sánchez, S/N, La Laguna, Tenerife, 38203, Islas Canarias, Spain.

** Corresponding author.

*** Corresponding author.

**** Corresponding author. Instituto Universitario de Enfermedades Tropicales y Salud Pública de Canarias, Universidad de La Laguna, Avda. Astrofísico Fco. Sánchez, S/N, La Laguna, Tenerife, 38203, Islas Canarias, Spain.

E-mail addresses: dtejedor@ipna.csic.es (D. Tejedor), jpinero@ull.edu.es (J.E. Piñero), jmlorenz@ull.edu.es (J. Lorenzo-Morales).

[1] Both authors contributed equally to this work.

https://doi.org/10.1016/j.ijpddr.2021.09.004

Received 7 September 2021; Received in revised form 24 September 2021; Accepted 28 September 2021

Available online 2 October 2021

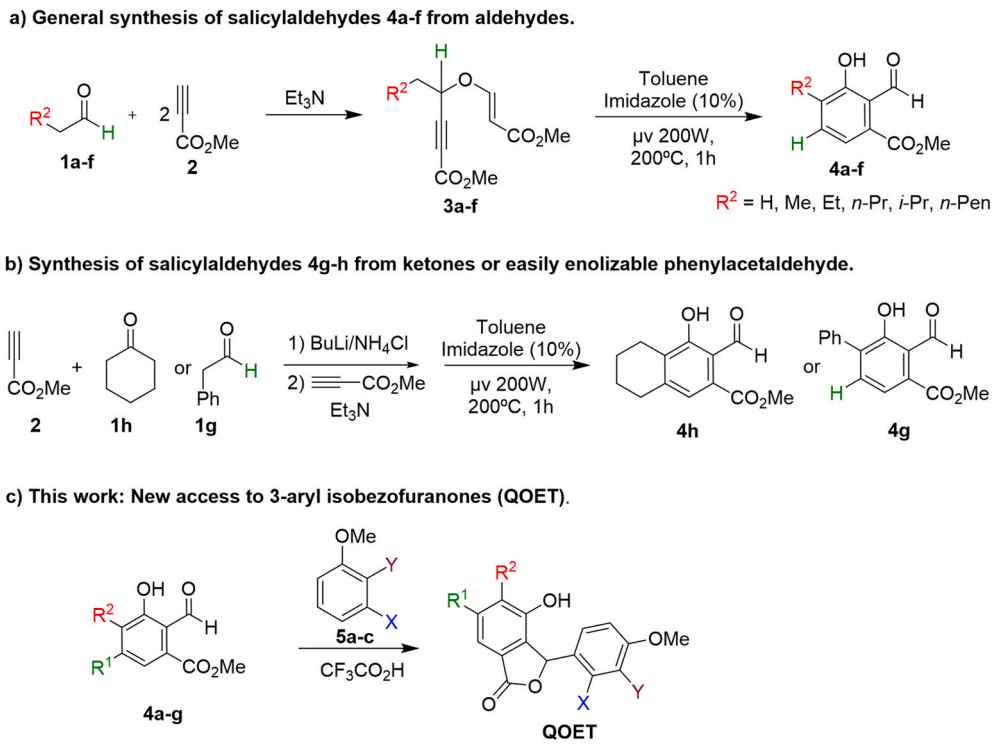

Fig. 1. a) General synthesis of salicylaldehydes **4a-f** from aldehydes. b) Synthesis of salicylaldehydes **4g-h** from ketones or easily enolizable phenylacetaldehyde. c) New access to 3-aryl isobezofuranones. μυ = microwave irradiation.

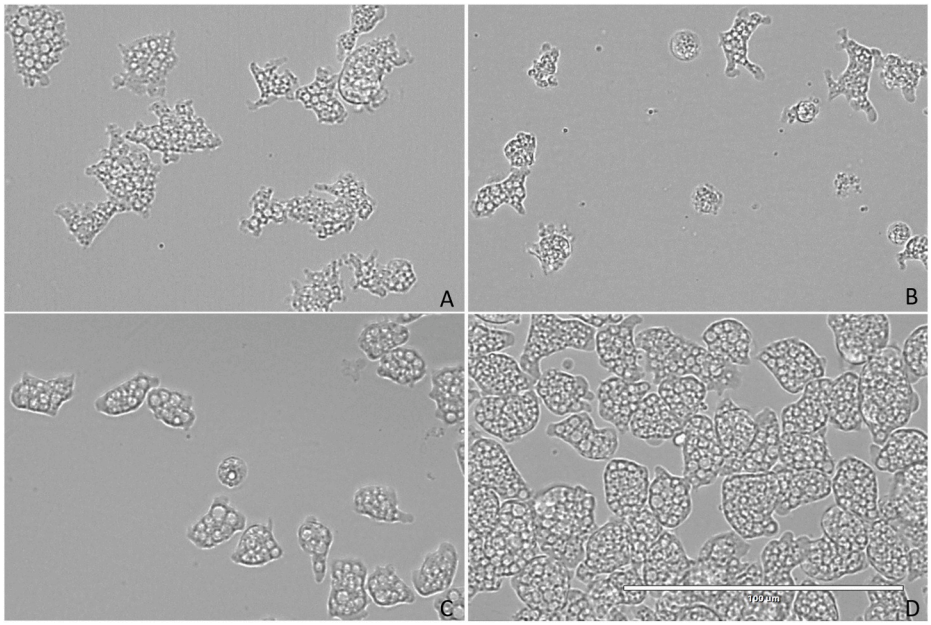

Fig. 2. Growth inhibition of N. fowleri (ATCC 30808) trophozoites at 48 h at IC_{50} concentration. QOET1 (**A**), QOET3 (**B**), QOET34 (**C**) and Negative control (**D**). All images (**x40**) are representative of the population of treated amoeba and are based on the live cell imaging microscope EVOS FL cell imaging system.

present time it has been classified as a B category priority pathogen by the National Institute of Allergy and Infectious Diseases (NIAID) (Tillery et al., 2021).

Primary Amoebic Encephalitis (PAM), that mainly affects healthy children and young adults, presents mortality rates above 95% of the registered cases (Bellini et al., 2020; Graciaa et al., 2018b; Siddiqui et al., 2016), being designated as a rapid and fulminant disease (Betanzos et al., 2019; Cope and Ali, 2016; Lopez et al., 2012). *Naegleria fowleri* is commonly isolated in untreated water sources, including hot water springs or poorly maintained swimming pools (Yoder et al., 2010). The infection is produced after carrying out careless activities (Bellini et al., 2020; De Jonckheere, 2011; Graciaa et al., 2018b; Yoder et al., 2012) when the trophozoite penetrates the nasal cavity. Once the amoeba is in the olfactory nerve, it migrates and penetrates the cribriform plate, invading the central nervous system (CNS) (Betanzos et al., 2019; Jahangeer et al., 2020). The infection produces an extensive parenchymal inflammation and haemorrhagic necrosis (Aitor Rizo-Liendo et al., 2020a). Symptomatology, which is not specific for

PAM cases, appears from 1 to 9 days after exposure, showing seizures, fever or bi-frontal headache in early stages of infection, and hallucinations, paralysis and leading to coma in later stages (Arberas-Jiménez et al., 2020; Trabelsi et al., 2012). Due to the non-existence of specific symptomatology of PAM, the quick development of the disease (from 1 to 18 days between the detection of the first symptoms to the death) (Maciver et al., 2020; Rizo-Liendo et al., 2019) and the lack of a rapid clinical detection method, the diagnosis of PAM cases is often undertaken post-mortem (Aitor Rizo-Liendo et al., 2020a).

In addition, with the absence of specific PAM therapy protocols the treatment of patients becomes an arduous challenge. Currently the experimental therapy options involve Amphotericin B (Amp B) and Miltefosine, alone or in combination with other drugs (rifampin, azithromycin or azoles) or with hypothermia, reporting successful results in PAM cases (Grace et al., 2015; Heggie and Küpper, 2017; Aitor Rizo-Liendo et al., 2020b), but also showing, undesired toxic side effects, such as in patients treated with Amp B that showed nephrotoxicity, anaemia or even brain damage (Laniado-Laborín and Cabrales-Vargas, 2009; Rizo-Liendo et al., 2019). Consequently, there is a correlation between the high mortality rate data with the late diagnosis and the non-specific treatment (Cope and Ali, 2016). Hence, the development of novel amoebicidal compounds (fast action, more efficiently and with low toxic effects) is an urgent need (Zeouk et al., 2021).

Isobenzofuranones or phthalides are a small group of natural molecules which have been isolated from different plants and/or fungi (Sánchez-Fernández et al., 2020). Moreover, these molecules have been reported as the main bioactive compounds in some of the plants used in the traditional medicine in Asia, European and North America (León et al., 2017). Previous studies have shown several biological properties of these molecules such as antibacterial (Rahman et al., 2005), antitumoral (Da Silva Maia et al., 2016; Logrado et al., 2010; Teixeira et al., 2013) and antifungal activities (Sánchez-Fernández et al., 2020; Strobel et al., 2002). In addition, a recent study in *Leishmania* genus, a parasitic protozoan, showed the activity of isobenzofuranones against this pathogen(Mishra et al., 2014; Pereira et al., 2015).

On the other hand, although there are different approaches to the synthesis of 3-aryl substituted isobezofuranones (Carlos et al., 2019; Chang et al., 2007; Hu et al., 2014; Huang et al., 2019; Lu et al., 2017; Mal et al., 2007; Phan et al., 2009; Touchet et al., 2018; Xing et al., 2010; Yang and Yoshikai, 2014; Yohda and Yamamoto, 2015), we wanted to take advantage of our previously reported access to polysubstituted salicylaldehydes (Tejedor et al., 2011, 2015, 2016) to design a rapid entry to a small library of this type of substrates. This strategy consists on the synthesis of propargyl vinyl ethers (PVEs) from methyl propiolate and different aldehydes or ketones (De Armas et al., 2001; León et al., 2010; Tejedor et al., 2003), their subsequent transformation into functionalized salicylaldehydes via a microwave assisted domino reaction triggered by a propargyl Claisen rearrangement, and finally, the metal-free and straightforward generation of the corresponding isobenzofuranones via their acid-catalyzed reaction with electron-rich arenes (Fig. 1). Subsequently, we built a small library of 14 different isobenzofuranones QOET from seven different carbonyl compounds (**1a-f**, **2**) and three different electron rich arenes (**5a-c**).

The aim of this study was to evaluate the anti-*Naegleria* activity of the isobenzofuranones that compose the library mentioned above (Fig. 1).

2. Material and methods

2.1. Chemicals

^{1}H NMR and ^{13}C NMR spectra of $CDCl_3$ solutions were recorded either at 400 and 100 MHz or at 500 and 125 MHz (Bruker Ac 200 and AMX2-500), respectively. Mass spectra (low resolution) (EI/CI) were obtained with a Hewlett-Packard 5995 gas chromatograph/mass spectrometer. High-resolution mass spectra were recorded with a mass spectrometer LCT Premier XE with two types of ionization sources: electrospray (ESI), an atmospheric pressure chemical ionization source (APCI), and with an orthogonal acceleration time-of-flight (oa-TOF) analyzer. Analytical thin-layer chromatography plates used were E. Merck Brinkman UV-active silica gel (Kieselgel 60 F254) on aluminum. Flash column chromatography was carried out with E. Merck silica gel 60 (particle size less than 0.020 mm) using appropriate mixtures of ethyl acetate in hexane unless other solvents are specified. All reactions were performed in oven-dried glassware. All materials were obtained from commercial suppliers and used as received. Reactions were stirred under the given conditions using a hotplate stirrer with a Heat-On™ Block System. The synthesis of intermediates 3 and 4 has been previously described (Tejedor et al., 2011, 2015, 2016).

2.2. General procedure for the synthesis of isobenzofuranones

The appropriate salicylaldehyde (2.0 mmol) and the corresponding methoxybenzene (2.6 mmol) were dissolved in 3 mL of trifluoroacetic acid and heated under reflux for 48 h. After the solvent was removed by rotary evaporation under reduced pressure, CH_2Cl_2 and water were added, and the organic phase was separated and dried over anhydrous Na_2SO_4. The residue was purified by flash column chromatography using AcOEt/hexane (10/90) as the eluent.

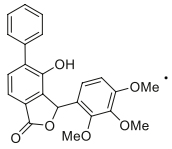

. **QOET-1:** ^{1}H NMR ($CDCl_3$, 400 MHz): δ = 3.84 (s, 3H), 3.87 (s, 3H), 4.09 (s, 3H), 6.67 (s, 1H), 6.70 (d, 1H, *J* = 8.8 Hz), 6.91 (d, 1H, *J* = 8.8 Hz), 7.35–7.39 (m, 1H), 7.41–7.45 (m, 4H), 7.48–7.50 (m, 2H), 7.54 (d, 1H, *J* = 7.8 Hz). ^{13}C NMR ($CDCl_3$, 100 MHz): δ = 56.1, 60.1, 62.0, 76.0, 108.7, 117.4, 120.9, 121.0, 125.8, 128.1, 128.6 (2C), 129.2 (2C), 132.6, 134.6, 135.6, 136.6, 141.9, 147.9, 149.3, 154.4, 170.5 ppm. HRMS (ESI$^+$): m/z [M+Na]$^+$ calculated for $C_{23}H_{20}O_6$ 415.1158, found 415.1160.

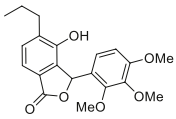

. **QOET-2:** ^{1}H NMR ($CDCl_3$, 400 MHz): δ = 0.93 (t, 3H, *J* = 7.2 Hz), 1.55–1.67 (m, 2H), 2.52–2.59 (m, 1H), 2.63–2.70 (m, 1H), 3.84 (s, 3H), 3.90 (s, 3H), 4.17 (s, 3H), 6.58 (s, 1H), 6.70 (d, 1H, *J* = 8.8 Hz), 6.92 (d, 1H, *J* = 8.8 Hz), 7.24 (d, 1H, *J* = 7.6 Hz), 7.39 (d, 1H, *J* = 7.6 Hz), 7.71 (s, 1H). ^{13}C NMR ($CDCl_3$, 100 MHz): δ = 14.0, 22.6, 32.3, 56.1, 61.0, 62.3, 75.4, 109.1, 117.1, 120.3, 121.3, 123.6, 131.8, 134.6, 136.6, 141.8, 148.3, 148.8, 154.1, 170.9 ppm. HRMS (ESI$^+$): m/z [M+Na]$^+$ calculated for $C_{20}H_{22}O_6$ 381.1314, found 381.1310.

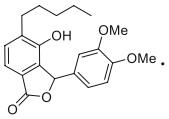

. **QOET-3:** ^{1}H NMR ($CDCl_3$, 400 MHz): δ = 0.87 (t, 3H, *J* = 6.5 Hz), 1.27–1.35 (m, 4H), 1.55–1.63 (m, 2H), 2.57–2.70 (m, 2H), 3.77 (s, 3H), 3.80 (s, 3H), 4.84 (bs, 1H), 6.31 (s,1H), 6.71 (d, 1H, *J* = 1.8 Hz), 6.84 (d, 1H, *J* = 8.4 Hz), 6.94 (d, 1H, *J* = 8.4 Hz), 7.33 (d, 1H, *J* = 7.7 Hz), 7.47 (d, 1H, *J* = 7.7 Hz). ^{13}C NMR ($CDCl_3$, 100 MHz): δ = 13.9, 22.4, 29.3, 29.8, 31.5, 55.90, 55.92, 80.9, 110.5, 111.3, 117.8, 120.4, 125.4, 127.1, 132.2, 134.8, 136.2, 148.5, 149.7, 150.4, 170.5 ppm. HRMS (ESI$^+$): m/z [M+Na]$^+$ calculated for $C_{21}H_{24}O_5$ 379.1521, found 379.1524.

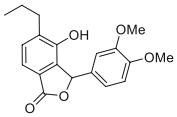

. **QOET-4:** ^{1}H NMR ($CDCl_3$, 400 MHz): δ = 0.94 (t, 3H, *J* = 7.3 Hz), 1.58–1.70 (m, 2H), 2.57–2.69 (m, 2H), 3.79 (s, 3H), 3.87 (s, 3H), 4.72 (s, 1H), 6.31 (s, 1H), 6.72 (d, 1H, *J* = 1.9 Hz), 6.86 (d, 1H, *J* = 8.2 Hz), 6.92 (dd, 1H, *J* = 8.2 Hz and 1.9 Hz), 7.33 (d, 1H, *J* =

7.6 Hz), 7.49 (d, 1H, $J = 7.6$ Hz). ^{13}C NMR ($CDCl_3$, 100 MHz): δ = 13.8, 22.8, 31.7, 55.93, 55.95, 80.8, 110.3, 111.3, 117.8, 120.4, 125.4, 127.1, 132.3, 134.7, 135.8, 148.4, 149.7, 150.4, 170.3 ppm. HRMS (ESI$^+$): m/z $[M+Na]^+$ calculated for $C_{19}H_{20}O_5$ 351.1208, found 351.1209.

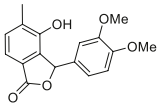

. **QOET-5:** ^{1}H NMR ($CDCl_3$, 500 MHz): δ = 2.30 (s, 3H), 3.79 (s, 3H), 3.86 (s, 3H), 4.85 (bs, 1H), 6.30 (s, 1H), 6.73 (d, 1H, $J = 2.0$ Hz), 6.85 (d, 1H, $J = 8.1$ Hz), 6.91 (dd, 1H, $J = 8.1$ Hz and 2.0 Hz), 7.33 (d, 1H, $J = 7.6$ Hz), 7.46 (d, 1H, $J = 7.6$ Hz). ^{13}C NMR ($CDCl_3$, 125 MHz): δ = 15.8, 55.9, 56.0, 80.8, 110.4, 111.3, 117.8, 120.3, 125.5, 127.2, 131.2, 133.0, 134.6, 148.7, 149.7, 150.4, 170.3 ppm. HRMS (ESI$^+$): m/z $[M+Na]^+$ calculated for $C_{17}H_{16}O_5$ 323.0895, found 323.0891.

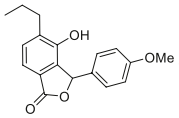

. **QOET-6:** ^{1}H NMR ($CDCl_3$, 400 MHz): δ = 0.95 (t, 3H, $J = 7.3$ Hz), 1.56–1.70 (m, 2H), 2.55–2.68 (m, 2H), 3.80 (s, 3H), 4.60 (s, 1H), 6.31 (s, 1H), 6.90 (d, 2H, $J = 8.5$ Hz), 7.22 (d, 2H, $J = 8.5$ Hz), 7.33 (d, 1H, $J = 7.6$ Hz), 7.48 (d, 1H, $J = 7.6$ Hz). ^{13}C NMR ($CDCl_3$, 125 MHz): δ = 13.9, 22.8, 31.7, 55.4, 80.5, 114.7 (2C), 117.8, 125.6, 126.6, 129.3 (2C), 132.2, 134.9, 135.6, 148.3, 160.9, 170.3 ppm. HRMS (ESI$^+$): m/z $[M+Na]^+$ calculated for $C_{18}H_{18}O_4$ 321.1103, found 321.1102.

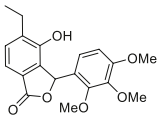

. **QOET-7:** ^{1}H NMR ($CDCl_3$, 400 MHz): δ = 1.19 (t, 3H, $J = 7.6$ Hz), 2.58–2.75 (m, 2H), 3.84 (s, 3H), 3.90 (s, 3H), 4.18 (s, 3H), 6.58 (s, 1H), 6.70 (d, 1H, $J = 8.8$ Hz), 6.92 (d, 1H, $J = 8.8$ Hz), 7.26 (d, 1H, $J = 7.8$ Hz), 7.40 (d, 1H, $J = 7.8$ Hz), 7.76 (s, 1H). ^{13}C NMR ($CDCl_3$, 100 MHz): δ = 13.7, 23.4, 56.1, 61.0, 62.3, 75.4, 109.1, 117.3, 120.3, 121.3, 123.6, 130.9, 134.5, 138.0, 141.9, 148.3, 148.7, 154.1, 170.9 ppm. HRMS (ESI$^+$): m/z $[M+Na]^+$ calculated for $C_{19}H_{20}O_6$ 367.1158, found 367.1155.

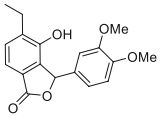

. **QOET-8:** ^{1}H NMR ($CDCl_3$, 400 MHz): δ = 1.22 (t, 3H, ^3J(H,H) = 7.4 Hz), 2.61–2.75 (m, 2H), 3.77 (s, 3H), 3.86 (s, 3H), 4.8 (bs, 1H), 6.32 (s, 1H), 6.72 (d, 1H, ^3J(H,H) = 1.9 Hz), 6.84 (d, 1H, ^3J(H,H) = 8.2 Hz), 6.90 (dd, 1H, ^3J(H,H) = 8.2 Hz and 1.9 Hz), 7.35 (d, 1H, ^3J(H,H) = 7.7 Hz), 7.48 (d, 1H, ^3J(H,H) = 7.7 Hz). ^{13}C NMR ($CDCl_3$, 125 MHz): δ = 13.8, 22.9, 55.90, 55.94, 80.9, 110.4, 111.2, 117.9, 120.4, 125.3, 127.1, 131.4, 134.7, 137.4, 148.3, 149.7, 150.3, 170.5 ppm. HRMS (ESI$^+$): m/z $[M+Na]^+$ calculated for $C_{18}H_{18}O_5$ 337.1052, found 337.1060.

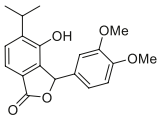

. **QOET-9:** ^{1}H NMR ($CDCl_3$, 500 MHz): δ = 1.25 (dd, 6H, $J = 6.9$ Hz and 1.5 Hz), 3.20–3.29 (m, 1H), 3.78 (s, 3H), 3.87 (s, 3H), 4.85 (bs, 1H), 6.31 (s, 1H), 6.72 (d, 1H,$J = 1.9$ Hz), 6.86 (d, 1H, $J = 8.2$ Hz), 6.92 (dd, 1H, $J = 8.2$ Hz and 2.0 Hz), 7.42 (d, 1H, $J = 8.0$ Hz), 7.52 (d, 1H, $J = 8.0$ Hz). ^{13}C NMR ($CDCl_3$, 100 MHz): δ = 22.3, 22.6, 27.1, 55.9, 56.0, 80.8, 110.4, 111.4, 118.1, 120.4, 125.0, 127.0, 128.6, 134.7, 141.8, 147.7, 149.8, 150.5, 170.3 ppm. HRMS (ESI$^+$): m/z $[M+Na]^+$ calculated for $C_{19}H_{20}O_5$ 351.1208, found 351.1207.

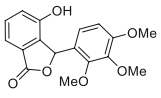

. **QOET-10:** ^{1}H NMR ($CDCl_3$, 400 MHz): δ = 3.83 (s, 3H), 3.89 (s, 3H), 4.16 (s, 3H), 6.61 (s, 1H), 6.70 (d, 1H, $J = 8.6$ Hz), 6.90 (d, 1H, $J = 8.6$ Hz), 7.06 (d, 1H, $J = 8.0$ Hz), 7.37 (t, 1H, $J = 7.7$ Hz), 7.46 (d, 1H, $J = 7.5$ Hz), 7.77 (s, 1H). ^{13}C NMR ($CDCl_3$, 100 MHz): δ = 56.1, 61.0, 62.3, 75.7, 109.0, 117.4, 120.3, 121.1, 121.9, 126.2, 131.1, 134.7, 142.0, 148.4, 151.3, 154.2, 170.7 ppm. HRMS (ESI$^+$): m/z $[M+Na]^+$ calculated for $C_{17}H_{16}O_6$ 339.0845, found 339.0844.

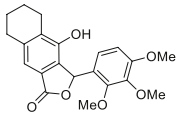

. **QOET-33:** ^{1}H NMR ($CDCl_3$, 400 MHz): δ = 1.72–1.81 (m, 4H), 2.62–2.70 (m, 2H), 2.75–2.83 (m, 2H), 3.83 (s, 3H), 3.89 (s, 3H), 4.17 (s, 3H), 6.55 (s, 1H), 6.69 (d, 1H, $J = 8.8$), 6.91 (d, 1H, $J = 8.8$), 7.21 (s, 1H), 7.75 (s, 1H). ^{13}C NMR ($CDCl_3$, 100 MHz): δ = 16.3, 56.1, 61.0, 62.3, 75.3, 109.0, 117.0, 120.2, 121.2, 123.7, 132.2, 132.5, 134.3, 141.8, 148.3, 149.0, 154.1, 170.9. HRMS (ESI$^+$): m/z $[M+Na]^+$ calculated for $C_{21}H_{22}O_6$ 393.1314, found 393.1317.

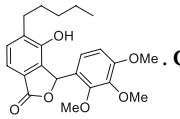

. **QOET-34:** ^{1}H NMR ($CDCl_3$, 400 MHz): δ = 0.86 (t, 3H, $J = 6.5$ Hz), 1.29–1.33 (m, 4H), 1.51–1.61 (m, 2H), 2.56 (ddd, 1H, $J = 15.6$, 9.1, 6.4), 2.67 (ddd, 1H, $J = 15.4$, 9.1, 6.4), 3.83 (s, 3H), 3.89 (s, 3H), 4.17 (s, 3H), 6.58 (s, 1H), 6.70 (d, 1H, $J = 8.8$), 6.91 (d, 1H, $J = 8.8$), 7.24 (d, 1H, $J = 7.6$), 7.38 (d, 1H, $J = 7,6$), 7.71 (s, 1H). ^{13}C NMR ($CDCl_3$, 100 MHz): δ = 14.0, 22.5, 29.1, 30.2, 31.7, 56.0, 61.0, 62.3, 75.4, 109.0, 117.1, 120.3, 121.2, 123.6, 131.7, 134.6, 136.8, 141.8, 148.3, 148.7, 154.1, 170.9 ppm. HRMS (ESI$^+$): m/z $[M+Na]^+$ calculated for $C_{22}H_{26}O_6$ 409.1627, found 409.1618.

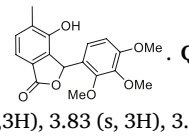

. **QOET-35:** ^{1}H NMR ($CDCl_3$, 400 MHz): δ = 2.25 (s,3H), 3.83 (s, 3H), 3.89 (s, 3H), 4.17 (s, 3H), 6.57 (s, 1H), 6.69 (d, 1H, $J = 8.8$), 6.90 (d, 1H, $J = 8.8$), 7.24 (d, 1H, $J = 7.6$), 7.36 (d, 1H, $J = 7,6$), 7.80 (s, 1H). ^{13}C NMR ($CDCl_3$, 100 MHz): δ = 22.36, 22.42, 23.7, 29.9, 56.1, 61.0, 62.3, 75.3, 109.1, 117.6, 120.1, 121.7, 122.4, 131.1, 131.7, 140.9, 141.8, 148.2, 148.4, 154.0, 171.2 ppm. HRMS (ESI$^+$): m/z $[M+Na]^+$ calculated for $C_{18}H_{18}O_6$ 353.1001, found 353.1008.

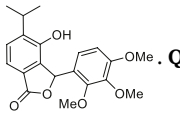

. **QOET-36:** ^{1}H NMR ($CDCl_3$, 400 MHz): δ = 1,19 (d, 3H, $J = 6.9$), 1.21 (d, 3H, $J = 6.9$), 3.29–3.37 (m, 1H), 3.83 (s, 3H), 3.90 (s, 3H), 4.17 (s, 3H), 6.58 (s, 1H), 6.70 (d, 1H, $J = 8.8$), 6.92 (d, 1H, $J = 8.8$), 7.33 (d, 1H, $J = 7.6$), 7.43 (d, 1H, $J = 7.6$), 7.74 (s, 1H). ^{13}C NMR ($CDCl_3$, 100 MHz): δ = 22.0, 22.7, 27.0, 56.1, 61.0, 62.3, 75.4, 109.0, 117.3, 120.3, 121.2, 123.3, 128.0, 134.6, 141.8, 142.3, 148.1, 148.3, 154.1, 170.9 ppm. HRMS (ESI$^+$): m/z $[M+Na]^+$ calculated for $C_{20}H_{22}O_6$ 381.1314, found 381.1315.

2.3. *Naegleria fowleri* cultures and cell line maintenance

Two type strains of *Naegleria fowleri* with reference number (ATCC® 30808™ and ATCC® 30215™) from the American Type Culture Collection (LG Promochem, Barcelona, Spain) were used in this study. Both strains were axenically cultured in 2% (w/v) Bactocasitone medium (Thermo Fisher Scientific, Madrid, Spain) at 37 °C, supplemented with 10% (v/v) of foetal bovine serum (FBS), containing 0,3 μg/mL of Penicillin G Sodium Salt and 0,5 mg/mL of Streptomycin sulphate (Sigma-Aldrich, Madrid, Spain). Amoebic strains were cultured in a biological security facility level 3 at the Instituto Universitario de Enfermedades Tropicales y Salud Pública de Canarias, Universidad de La Laguna, regarding to the Spanish biosafety guidelines for this pathogen (Rizo-Liendo et al., 2019).

For the cytotoxicity assays, the murine macrophage J774A.1 (ATCC

Table 1
[a] Yields for isolated pure compounds.[b] Recovered unreacted starting material.

ENTRY	4	R^2	R^1	X	Y	Yield (%)[a]	4 (rec %)[b]	QOET
1	**4a**	H	H	OMe	OMe	63	–	**QOET-10**
2	**4b**	Me	H	OMe	OMe	79	20	**QOET-35**
3	**4c**	Et	H	OMe	OMe	75	–	**QOET-7**
4	**4d**	*n*-Pr	H	OMe	OMe	73	–	**QOET-2**
5	**4e**	*i*-Pr	H	OMe	OMe	68	21	**QOET-36**
6	**4f**	*n*-Pen	H	OMe	OMe	88	–	**QOET-34**
7	**4g**	Ph	H	OMe	OMe	73	–	**QOET-1**
8	**4h**	Cyhex		OMe	OMe	22	49	**QOET-33**
9	**4b**	Me	H	H	OMe	50	–	**QOET-5**
10	**4c**	Et	H	H	OMe	49	–	**QOET-8**
11	**4d**	n-Pr	H	H	OMe	50	23	**QOET-4**
12	**4e**	*i*-Pr	H	H	OMe	55	14	**QOET-9**
13	**4f**	*n*-Pen	H	H	OMe	66	–	**QOET-3**
14	**4d**	*n*-Pr	H	H	H	22	–	**QOET-6**

TIB-67) cell line was used. The cells were cultured in Dulbecco's Modified Eagle's medium (DMEM, w/v) supplemented with 10% (v/v) FBS and 10 μg/mL gentamicin (Sigma-Aldrich, Madrid, Spain), at 37 °C in a 5% $C0_2$ atm (Sifaoui et al., 2017).

2.4. In vitro activity assays against Naegleria fowleri trophozoites

The *in vitro* activity of the isobenzofuranones included in this study was determined using a colorimetric assay based on the AlamarBlue® reagent as previously described (Rizo-Liendo et al., 2019). The trophozoites, from a stock solution of $2*10^5$ cells/ml, were seeded in duplicate (50 μl) on a 96-microtiter plate (Thermo Fisher Scientific, Madrid, Spain). Then, 50 μl of a serial dilution of the tested compounds (in the same medium as *Naegleria fowleri*) was added to the plate. For the negative control, 50 μl of the medium alone was added to the seeded trophozoites. After that, the AlamarBlue® reagent (10% of the medium volume) was placed in each well and the plates were incubated with slight agitation at 37 °C for 48 h. Finally, plates were analysed with the EnSpire Multimode Plate Reader (PerkinElmer, Madrid, Spain) using a wavelength of excitation of 570 nm and a reference wavelength of 630 nm.

The percentages of growth inhibition and 50% and 90% inhibitory concentrations (IC_{50} and IC_{90}) were calculated performing a no linear regression analysis with a 95% confidence limit using the GraphPad Prism8.0.2 software program (GraphPad Software, San Diego, CA, USA). All activity experiments were made in triplicate and the mean values were also calculated. A paired two-tailed *t*-test was used for the analysis of the data and the values of $P < 0.05$ were considered as statistically significant.

2.5. Cytotoxicity assays

The cytotoxic concentration 50 (CC_{50}) of the tested compounds was evaluated using a murine macrophages cell line J774A.1 (ATCC® TIB-67™). Briefly, different concentrations of the compounds were incubated with the cells (from a stock solution of 10^5 cells/ml) and the AlamarBlue® (10% of the medium volume) reagent was added to each well. As a negative control, 50 μl of the medium alone was added to the seeded cells. The plates were incubated for 24 h at 37 °C in a 5% CO_2 atmosphere (Lorenzo-Morales et al., 2015; Sifaoui et al., 2017).

2.6. Evaluation of the programmed cell death induction (PCD) in Naegleria fowleri

The ATCC® 30808™ *Naegleria fowleri* strain was used to carry out the assessment of the programmed cell death induction by the most promising molecules in the trophozoites forms.

2.6.1. Double stain assay for detection of chromatin condensation

A double-stain apoptosis detection kit (Hoechst 33342/PI) (Life Technologies, Madrid, Spain) and an EVOS FL Cell Imaging System AMF4300, (Life Technologies, Madrid, Spain) were used to perform the detection of chromatin condensation, following manufacturer's instructions. Briefly, $5*10^5$ cells/ml were incubated with the previously calculated IC_{90} of the compounds during 24 h at 37 °C.

This kit allows to distinguish between three different cell populations: death cells will show an intense red fluorescence (as the PI stain enters the nucleus), cells undergoing PCD will show blue fluorescence (as the Hoechst 33342 stain bind the condensed chromatin) and live cells will show a low blue fluorescence (Sifaoui et al., 2018).

2.6.2. Plasma membrane permeability evaluation

In order to evaluate the permeability of the cell membrane the SYTOX Green assay (Life Technologies, Madrid, Spain) was performed. Firstly, amoebae from a stock solution of $5*10^5$ cells/ml were incubated

Table 2
Inhibitory concentrations (IC_{50}/IC_{90}) of the evaluated isobenzofuranones against the trophozoite stage of Naegleria fowleri type strains ATCC® 30808™ and ATCC® 30215™, and cytotoxicity values (CC_{50}) against murine macrophages J774A.1 strain ATCC® TIB-67™. N/A indicates that no activity was observed. N/D indicates that values were not determined. The selectivity index (SI) of the active compounds was also calculated.

Compound	N. fowleri ATCC® 30808™ IC_{50} (μM)	N. fowleri ATCC® 30215™ IC_{50} (μM)	Murine macrophage J774.A1 CC_{50} (μM)	N. fowleri ATCC® 30808™ SI* (CC_{50}/IC_{50})	N. fowleri ATCC® 30215™ SI* (CC_{50}/IC_{50})	N. fowleri ATCC® 30808™ IC_{90} (μM)
QOET-1	17.42 ± 5.02	12.89 ± 1.68	≥509.68	≥29.26	≥39.51	103.06
QOET-2	58.97 ± 9.54	N/D	94.45 ± 3.57	1.60	N/D	N/D
QOET-3	19.88 ± 5.29	12.99 ± 2.47	≥561.17	≥28.23	≥43.20	93.49
QOET-4	N/A	N/D	≥152.25	N/D	N/D	N/D
QOET-5	N/A	N/D	≥333.00	N/D	N/D	N/D
QOET-6	N/A	N/D	≥335.23	N/D	N/D	N/D
QOET-7	N/A	N/D	≥290.44	N/D	N/D	N/D
QOET-8	≥318.17	N/D	≥159.08	≥0.50	N/D	N/D
QOET-9	89.07 ± 13.55	34.88 ± 4.84	≥304.60	≥3.42	≥8.73	N/D
QOET-10	N/A	N/D	≥316.16	N/D	N/D	N/D
QOET-33	90,93 ± 5,67	N/D	≥134.99	≥1.49	N/D	N/D
QOET-34	27,67 ± 1,99	7.79 ± 0.88	≥129.40	≥4.68	≥16.61	56.08
QOET-35	99,24 ± 6,69	N/D	≥151.33	≥1.52	N/D	N/D
QOET-36	95,23 ± 0,56	N/D	≥139.51	≥1.47	N/D	N/D
Amphotericin B	0.121 ± 0.032	0.166 ± 0.026	≥200	≥1652.893	≥1204.819	–
Miltefosine	38.742 ± 4.232	81.574 ± 7.236	127.887 ± 8.852	3.301	1.568	–

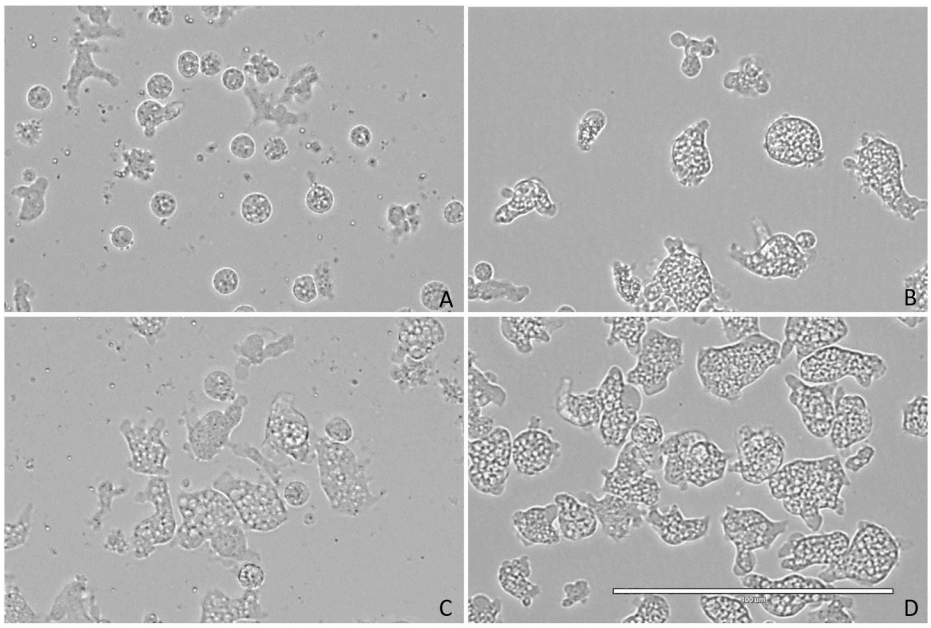

Fig. 3. N. fowleri (ATCC30215) trophozoites incubated with the IC_{50} of QOET1 (**A**), QOET3 (**B**), QOET34(**C**) and Negative control (**D**). All images (**x40**) are representative of the population of treated amoeba and are based on the live cell imaging microscope EVOS FL cell imaging system.

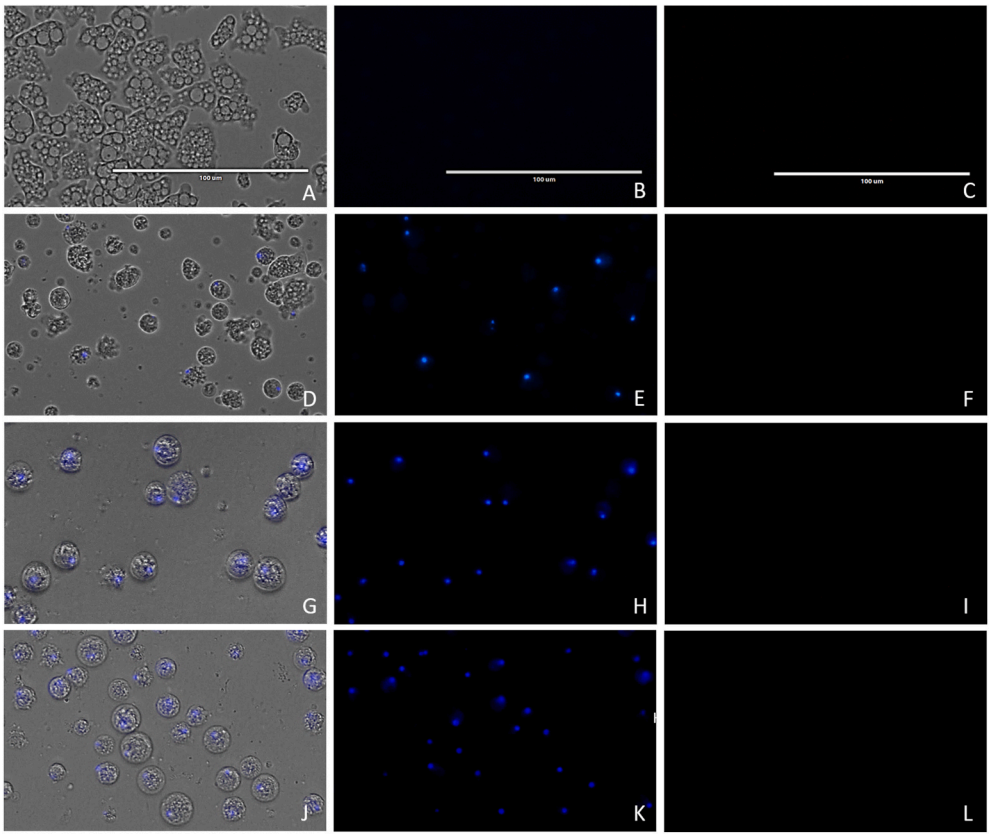

Fig. 4. Naegleria fowleri trophozoites incubated with IC_{90} of the evaluated compounds for 24 h (D–L). Negative control (A–C), QOET1 (D–F), QOET3 (G–I) and QOET34 (J–L). The results of the Hoechst stain is different in control cells, where no fluorescence is observed (B), and in treated cells, where the nuclei are intense blue (E,H,K). Overlay channel (A,D,G,J); Hoechst channel (B,E,H,K), and propidium iodide channel (C, F,I,L). Images (40 ×) are representative of the cell population observed in the performed experiments. Images were obtained using an EVOS FL Cell Imaging System AMF4300, Life Technologies, USA. (For interpretation of the references to color in this figure legend, the reader is referred to the Web version of this article.)

in a 96-well plate with the IC_{90} of the selected molecules. After 24 h, the Sytox Green dye was added at a final concentration of 1 μM and incubated for 15 min to finally observe the cells in an EVOS FL Cell Imaging System AMF4300 (Life Technologies, Madrid, Spain). Sytox Green dye binds DNA and shows high green fluorescence when the membrane is permeable and enables it to enter the cytoplasm (Lorenzo-Morales et al., 2019).

2.6.3. Generation of intracellular reactive oxygen species (ROS)

The generation of ROS in treated amoebae was determined with the CellROX Deep Red fluorescent probe (Invitrogen, Termo Fisher Scientifc, Madrid, Spain). The experiment was carried out after incubating $5*10^5$ cells/ml with the IC_{90} of the tested compounds at 37 °C during 24 h. Afterwards, cells were exposed to CellROX Deep Red (final concentration 5 μM) and incubated for 30 min in dark. Finally, the presence or

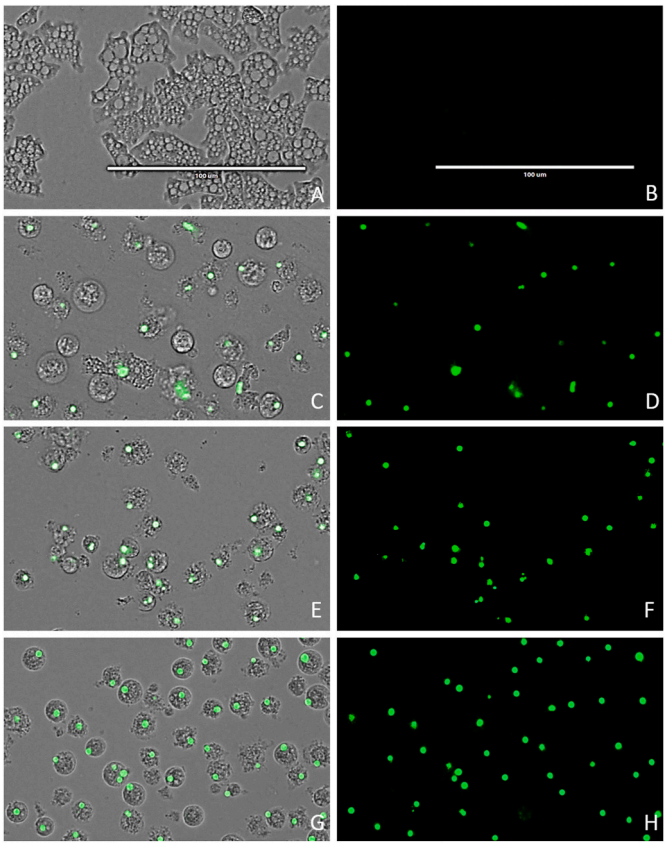

Fig. 5. Permeation of the Naegleria fowleri plasma membrane to the vital dye SYTOX green caused by addition of QOET1 (C,D), QOET3 (E,F) and QOET34 (G,H) at IC90 after 24 h. Negative Control (A,B). Images (40 ×) are representative of the cell population observed in the performed experiments. Images were obtained using an EVOS FL Cell Imaging System AMF4300, Life Technologies, Madrid, Spain. (For interpretation of the references to color in this figure legend, the reader is referred to the Web version of this article.)

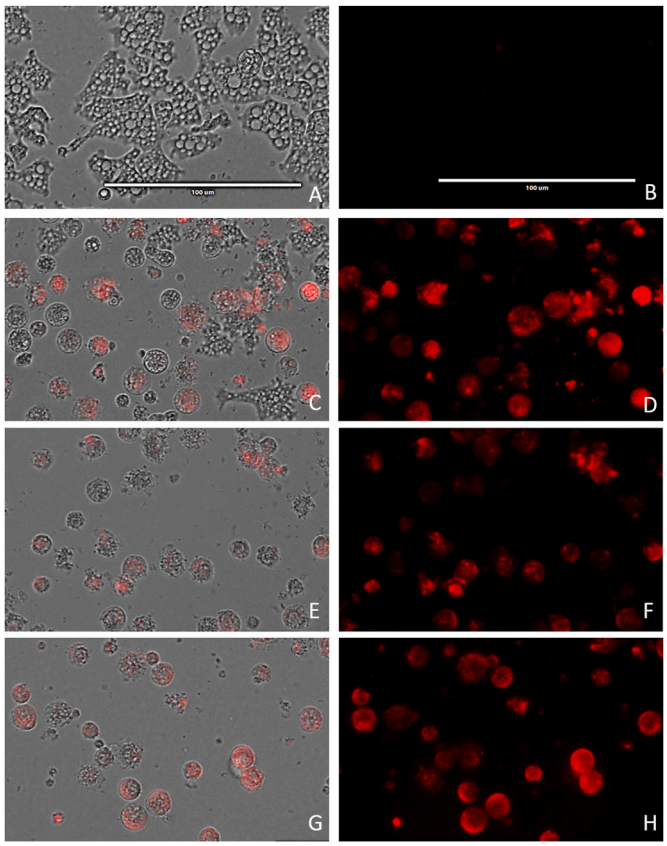

Fig. 6. Increase levels of intracellular ROS levels (red fluoresncence) caused by the addition of QOET1 (C and D), QOET3 (E and F) and QOET 34 (G and H) at IC_{90} after 24 h of incubation. Negative control (A and B) The evaluated compounds were added to the cells and exposed to CellROX® Deep Red (5 μM, 30 min) at 37 °C in the dark. Images (40×) are representative of the cell population observed in the performed experiments. Images were obtained using an EVOS FL Cell Imaging System AMF4300, Life Technologies, Spain. (For interpretation of the references to color in this figure legend, the reader is referred to the Web version of this article.)

ROS was evaluated with EVOS FL Cell Imaging System AMF4300 (Life Technologies, Madrid, Spain) as they show high red fluorescence (Arberas-Jiménez et al., 2020).

2.6.4. Analysis of mitochondrial function disruption

2.6.4.1. ATP level measurement. The Celltiter-Glo® Luminescent Cell Viability Assay (Promega Biotech Ibérica, Madrid, Spain) was used, following manufacturer's indications, to measure the ATP levels after treating the cells ($5*10^5$ cells/ml) with the IC_{90} of the compounds for 24 h, at 37 °C. An EnSpire® Multimode Plate Reader (PerkinElmer, Madrid, Spain) was used to obtain the luminescence data (Lorenzo-Morales et al., 2019). The experiment was carried out in triplicate. Briefly, after the previous mentioned incubation, reactive was added to the wells in 1:1 proportion. Afterwards 2 min of vigorous shake, plate was incubated in darkness for 10 min before the luminescence reading.

2.6.4.2. Mitochondrial membrane potential. The collapse of an electrochemical gradient across the mitochondrial membrane in the treated cells during PCD was evaluated using the JC-1 mitochondrial membrane potential detection kit (Cayman Chemicals, Vitro SA, Madrid, Spain). *Naegleria fowleri* trophozoites, from a stock solution of $5*10^5$ cells/ml, were incubated with the IC_{90} of the tested isobenzofuranones at 37 °C for 24 h and the assay was carried out following manufacturer's recommendations. The images were obtained with an EVOS FL Cell Imaging System AMF4300 (Life Technologies, Madrid, Spain). The obtained staining pattern permitted the identification of two groups in a cellular population: Healthy cells, that will show only red fluorescence, and cells presenting low mitochondrial membrane potential (undergoing PCD), which would show an intense level of green and red fluorescence (Aitor Rizo-Liendo et al., 2020a).

2.7. Statistical analysis

All data were recorded, edited, and entered using GraphPad Prism version 9.0 (GraphPad Software; CA; USA). The data are expressed as the mean ± standard deviation of at least three independent experiments. A statistical analysis was conducted using one-way analysis of variance (ANOVA). Statistical significance was set at $p < 0.05$.

3. Results

3.1. Synthesis of isobenzofuranones

As it can be extracted from Table 1, which shows the results for the synthesis of the small library of 14 different isobenzofuranones QOET, better efficiencies and good yields are obtained with the more electro-rich 1,2,3-trimethoxybenzene (entries 1–7) except for the more sluggish salicylaldehyde **4g** derived from cyclohexanone (entry 8). The reactions with 1,2-dimethoxybenzene affords moderate but acceptable yields of the desired isobenzofuranones (entries 9–13), while the reaction of anisole gives in comparison only a low yield of the final product

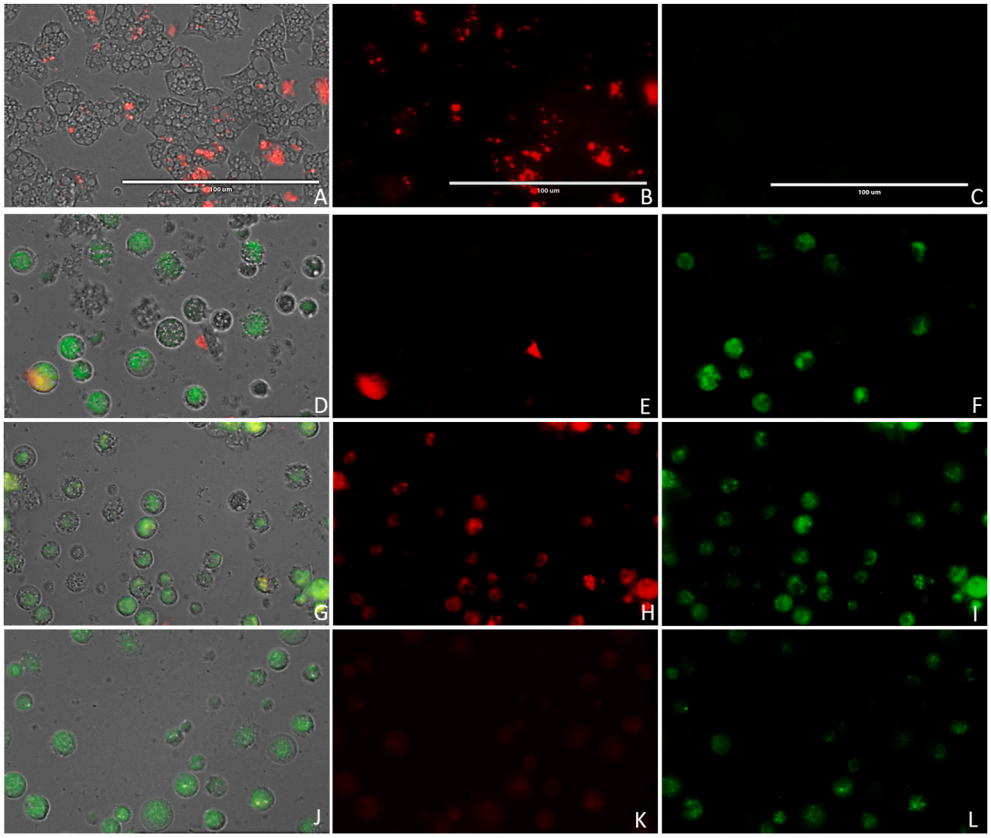

Fig. 7. Effect of QOET1 (D–F), QOET3 (G–I) and QOET34 (J–L) on the mitochondrial membrane potential. Negative control (A–C). The JC-1 dye accumulates in the mitochondria of healthy cells as aggregates and emits a red fluorescence (red channel: B, E,H,K). Cells treated with the IC90 of the compounds for 24 h emitted a green fluorescence (green channel: C,F,I,L); due to the decrease in mitochondrial membrane potential, the JC-1 remained in the cytoplasm in monomeric form and emit green fluorescence. Images (40×) are representative of the cell population observed in the performed experiments. Images were obtained using an EVOS FL Cell Imaging System AMF4300, Life Technologies, Spain. (For interpretation of the references to color in this figure legend, the reader is referred to the Web version of this article.)

QOET-6.

3.2. *In vitro activity and toxicity of isobenzofuranones against Naegleria fowleri*

In vitro activity assays revealed that 8 of the 14 isobenzofuranones included in this study were active against the *Naegleria fowleri* ATTC 30808® strain as shown in Table 2. Among them, QOET-1, QOET-3, QOET-9 and QOET-34 stand out for their inhibitory concentration 50 (IC_{50}) value (Fig. 2 and S29), being more active than miltefosine (one of the reference drugs).

Moreover, considering the *In vitro* activity showed against ATCC 30808 strain, 4 compounds were evaluated against a trophozoite stage of the clinical strain ATCC 30215, obtaining IC_{50} values ranging from 7.79 ± 0.88 μM to 34.88 ± 4.84 μM (Fig. 3 and S30). Consequently, QOET-1, QOET-3 and QOET-34 were selected as candidates to continue with the evaluation of the PCD induction in treated cells due to their low IC_{50} and toxicity levels.

3.3. *Evaluation of PCD induction in treated Naegleria fowleri trophozoites*

The chromatin condensation assay was positive for the three evaluated isobenzofuranones since the treated cells exhibited an intense blue fluorescent-stained nucleus as shown in Fig. 4 and S31, corresponding to condensed chromatin.

All the compounds caused plasma membrane damage when amoebas were treated with the IC_{90} after 24 h as an intense green fluorescence can be observed in Fig. 5 and S32.

The *Naegleria fowleri* trophozoites treated with IC_{90} of both QOET-1, QOET-3 or QOET-34 during 24 h showed an increase in the ROS production as it is visible in Fig. 6 and S33.

Evaluated compounds induced changes on mitochondrial inner membrane potential of the treated trophozoites since green fluorescence is shown, which corresponds to the monomeric form of the JC-1 dye (Fig. 7 and S34). In order to confirm these results, the ATP production after 24 h was also measured. The results showed that cells decreased their ATP levels in a 66.53% when treated with QOET-1, a 98.91% when treated with QOET-3 and a 67.06% when treated with QOET-34 comparing with the negative control (Fig. 8).

4. Discussion

In the present study, we evaluated the activity of 14 isobenzofuranone derivatives as potential anti-*Naegleria* compounds. The obtained results showed that three of the tested compounds were active at low concentrations ranging from 7.79 to 27.67 μM. Interestingly, the obtained IC_{50}s revealed that the selected isobenzofuranones were more active against the ATCC® 30215 strain (Table 2), which is more resistant to the current therapeutic agents used to treat PAM as it has been previously reported by our group and others(Rice et al., 2015; Rizo-Liendo et al., 2021).

Moreover, 3-butyl-6-bromo-1(3H)-isobenzofuranone (Br-NBP) showed short half-life, good dose-linear pharmacokinetic profile, wide tissue distribution, and different degree protein binding to various species plasma (Tian et al., 2016). In addition, these molecules have been proposed as good candidates for cancer therapy (Naik et al., 2012).

Programmed cell death and apoptosis-like processes have been described in different unicellular protozoan parasites(Kaczanowski et al., 2011). Moreover, previous studies have proved the induction of apoptosis-like process after the treatment of *Leishmania* spp. with isobenzofuranones(Mishra et al., 2014).

Cardenas-Zuñiga and colleagues described PCD process in *Naegleria fowleri* and *Naegleria gruberi* for the first time(Cárdenas-Zúñiga et al., 2017). In previous works of our group, PCD process in *Naegleria fowleri* was evaluated after detection of specific metabolic events such as DNA condensation, plasmatic membrane and mitochondrial membrane

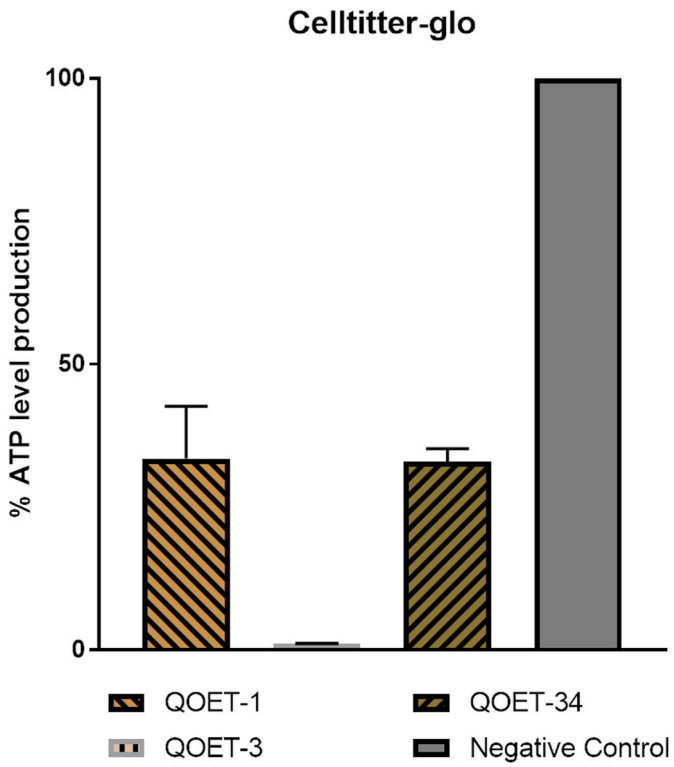

Fig. 8. ATP levels in relative percentages compared to the negative control in Naegleria fowleri trophozoites after 24 h of incubation with the IC90 of the evaluated molecules. The results show a decrease of ATP levels of 66.53% (QOET1), 98.91% (QOET3) and 67.06% (QOET34) compared to the negative control (cells without treatment). Results are representing in percentage relative to the negative control. Differences between the values were assessed using one-way analysis of variance (ANOVA). Data are presented as means ± SD. NS: not significant. ****: p value < 0.0001.

damage, collapse of ATP levels and intracellular ROS generation(A. Rizo-Liendo et al., 2020; Zeouk et al., 2020). The isobenzofuranones selected in this study were able to induce all the metabolic events mentioned above hence showing signs of PCD induction (early apoptosis) leading to a safer therapy if used in the near future. In addition, cell death induction by necrosis could cause undesired inflammation processes in the patient whereas PCD (apoptosis) events do not induce inflammation (Rizo-Liendo et al., 2020).

In addition, the mechanism of action of isobenzofuranones in *Naegleria fowleri* has not yet been evaluated. However, these compounds have been described as inhibitors of the DNA topoisomerase type II in *Leishmania* genus(Mishra et al., 2014). On the other hand, anti-acetylcholinesterase properties have been also recently stated in some fungi species(Abbod et al., 2020).

Recently, the genome data from *Naegleria fowleri* and *Naegleria gruberi*(Liechti et al., 2019; Mullican et al., 2018) has been made available in the database where the DNA topoisomerase II gene (https://www.uniprot.org/uniprot/A0A6A5BHC1) and the AchE-like enzymes genes has been described (i.e https://www.uniprot.org/uniprot/D2V1M1) (Arberas-Jiménez et al., 2020). Therefore, inhibition of these enzymes could lead to the activation of PCD process observed in this parasite. Hence, the elucidation of these mechanisms could be a useful pathway to follow.

5. Conclusion

To conclude, the selected isobenzofuranones showed high activity against the two different *Naegleria fowleri* strains included in this study inducing PCD processes and low toxicity. Therefore, these compounds could be good candidates for future *in vivo* assays to develop new PAM therapeutic protocols.

Author contributions

ARL, JLM, JEP, IS, IAJ designed the concept and organized the manuscript. All authors performed experimental assays. ARL, IAJ, DT and JLM wrote the manuscript. All authors edited the manuscript and discussed the final version.

Declaration of competing interest

The authors declare that the research was conducted in the absence of any commercial or financial relationships that could be construed as a potential conflict of interest.

Acknowledgments

This work was funded by PI18/01380 from Instituto de Salud Carlos III, Spain and RICET (RD16/0027/0001 project), from Programa Redes Temáticas de Investigación Cooperativa, FIS (Ministerio Español de Salud, Madrid, Spain) and FEDER. IS was funded by the Agustín de Bethancourt Programme (Cabildo de Tenerife, TFinnova Programme supported by MEDI and FDCAN funds). ARL and IAJ were funded by Agencia Canaria de Investigación, Innovación y Sociedad de la Información (ACIISI). Part of this research was funded by the Spanish Ministry of Science, Innovation and Universities (MICINN), State Research Agency (AEI) and the European Regional Development Funds (ERDF) (PGC2018-094503-B-C21).

Appendix A. Supplementary data

Supplementary data to this article can be found online at https://doi.org/10.1016/j.ijpddr.2021.09.004.

References

Abbod, M., Safaie, N., Gholivand, K., Mehrabadi, M., Bonsaii, M., 2020. Mode of action of 3-butylidene phthalide as a competent natural pesticide. Pestic. Biochem. Physiol. 164, 228–236. https://doi.org/10.1016/j.pestbp.2020.02.003.

Ali, M., Jamal, S.B., Farhat, S.M., 2020. Naegleria fowleri in Pakistan. Lancet Infect. Dis. 20, 27–28. https://doi.org/10.1016/S1473-3099(19)30675-9.

Arberas-Jiménez, I., García-Davis, S., Rizo-Liendo, A., Sifaoui, I., Reyes-Batlle, M., Chiboub, O., Rodríguez-Expósito, R.L., Díaz-Marrero, A.R., Piñero, J.E., Fernández, J.J., Lorenzo-Morales, J., 2020. Laurinterol from Laurencia johnstonii eliminates Naegleria fowleri triggering PCD by inhibition of ATPases. Sci. Rep. 10 https://doi.org/10.1038/s41598-020-74729-y.

Bellini, N.K., da Fonseca, A.L.M., Reyes-Batlle, M., Lorenzo-Morales, J., Rocha, O., Thiemann, O.H., 2020. Isolation of naegleria spp. from a brazilian water source. Pathogens 9, 90. https://doi.org/10.3390/pathogens9020090.

Bellini, N.K., Santos, T.M., da Silva, M.T.A., Thiemann, O.H., 2018. The therapeutic strategies against Naegleria fowleri. Exp. Parasitol. 187, 1–11. https://doi.org/10.1016/j.exppara.2018.02.010.

Betanzos, A., Bañuelos, C., Orozco, E., 2019. Host invasion by pathogenic amoebae: epithelial disruption by parasite proteins. Genes 10, 618. https://doi.org/10.3390/genes10080618.

Cárdenas-Zúñiga, R., Silva-Olivares, A., Villalba-Magdaleno, J.D.A., Sánchez-Monroy, V., Serrano-Luna, J., Shibayama, M., 2017. Amphotericin B induces apoptosis-like programmed cell death in Naegleria fowleri and Naegleria gruberi. Microbiol. 163, 940–949. https://doi.org/10.1099/mic.0.000500.

Carlos, A.M.M., Stieler, R., Lüdtke, D.S., 2019. Catalytic asymmetric synthesis of 3-aryl phthalides enabled by arylation-lactonization of 2-formylbenzoates. Org. Biomol. Chem. 17, 283–289. https://doi.org/10.1039/c8ob02872a.

Chang, H.T., Jeganmohan, M., Cheng, C.H., 2007. Highly efficient cyclization of o-iodobenzoates with aldehydes catalyzed by cobalt bidentate phosphine complexes: a novel entry to chiral phthalides. Chem. Eur J. 13, 4356–4363. https://doi.org/10.1002/chem.200601880.

Cope, J.R., Ali, I.K., 2016. Primary amebic meningoencephalitis: what have we learned in the last 5 Years? Curr. Infect. Dis. Rep. 18, 31. https://doi.org/10.1007/s11908-016-0539-4.

Da Silva Maia, A.F., Siqueira, R.P., De Oliveira, F.M., Ferreira, J.G., Da Silva, S.F., Caiuby, C.A.D., De Oliveira, L.L., De Paula, S.O., Souza, R.A.C., Guilardi, S., Bressan, G.C., Teixeira, R.R., 2016. Synthesis, molecular properties prediction and cytotoxic screening of 3-(2-aryl-2-oxoethyl)isobenzofuran-1(3H)-ones. Bioorg. Med. Chem. Lett 26, 2810–2816. https://doi.org/10.1016/j.bmcl.2016.04.065.

De Armas, P., García-Tellado, F., Marrero-Tellado, J.J., Tejedor, D., Maestro, M.A., Gonzalez-Platas, J., 2001. Alkynoates as a source of reactive alkylinides for aldehyde addition reactions. Org. Lett. 3 https://doi.org/10.1021/ol015951b, 1905–1907.

De Jonckheere, J.F., 2011. Origin and evolution of the worldwide distributed pathogenic amoeboflagellate Naegleria fowleri. Infect. Genet. Evol. 11, 1520–1528. https://doi.org/10.1016/j.meegid.2011.07.023.

Debnath, A., Hahn, H.J., Abagyan, R., Podust, L.M., Roy, S., Ali, I.K.M., 2020. HMG-CoA reductase inhibitors as drug leads against naegleria fowleri. ACS Chem. Neurosci. 11, 3089–3096. https://doi.org/10.1021/acschemneuro.0c00428.

Fowler, M., Carter, R.F., 1965. Acute pyogenic meningitis probably due to Acanthamoeba sp.: a preliminary report. Br. Med. J. 2, 734–742. https://doi.org/10.1136/bmj.2.5464.734-a.

Grace, E., Asbill, S., Virga, K., 2015. Naegleria fowleri: pathogenesis, diagnosis, and treatment options. Antimicrob. Agents Chemother. 59, 6677–6681. https://doi.org/10.1128/AAC.01293-15.

Graciaa, D.S., Cope, J.R., Roberts, V.A., Cikesh, B.L., Kahler, A.M., Vigar, M., Hilborn, E. D., Wade, T.J., Backer, L.C., Montgomery, S.P., Evan Secor, W., Hill, V.R., Beach, M. J., Fullerton, K.E., Yoder, J.S., Hlavsa, M.C., 2018a. Outbreaks associated with untreated recreational water — United States, 2000–2014. Am. J. Transplant. 18, 2083–2087. https://doi.org/10.1111/ajt.15002.

Graciaa, D.S., Cope, J.R., Roberts, V.A., Cikesh, B.L., Kahler, A.M., Vigar, M., Hilborn, E. D., Wade, T.J., Backer, L.C., Montgomery, S.P., Secor, W.E., Hill, V.R., Beach, M.J., Fullerton, K.E., Yoder, J.S., Hlavsa, M.C., 2018b. Outbreaks associated with untreated recreational water — United States, 2000–2014. MMWR Morb. Mortal. Wkly. Rep. 67, 701–706. https://doi.org/10.15585/mmwr.mm6725a1.

Heggie, T.W., Küpper, T., 2017. Surviving Naegleria fowleri infections: a successful case report and novel therapeutic approach. Trav. Med. Infect. Dis. 16, 49–51. https://doi.org/10.1016/j.tmaid.2016.12.005.

Henker, L.C., Cruz, R.A.S., da, Silva, da, F.S., Driemeier, D., Sonne, L., Uzal, F.A., Pavarini, S.P., 2019. Meningoencephalitis due to naegleria fowleri in cattle in southern Brazil. Rev. Bras. Parasitol. Vet. 28, 514–517. https://doi.org/10.1590/s1984-29612019021.

Hu, J., Qin, H.L., Xu, W., Li, J., Zhang, F., Zheng, H., 2014. TfOH-catalyzed synthesis of 3-aryl isoindolinones via a tandem reaction. Chem. Commun. 50, 15780–15783. https://doi.org/10.1039/c4cc06653g.

Huang, H., Wang, Y., Zong, H., Song, L., 2019. Catalytic asymmetric 1,2-Addition/Lactonization tandem reactions for the syntheses of chiral 3-Substituted phthalides using organozinc reagents. Appl. Organomet. Chem. 33, e4643 https://doi.org/10.1002/aoc.4643.

Jahangeer, M., Mahmood, Z., Munir, N., Waraich, U.e.A., Tahir, I.M., Akram, M., Ali Shah, S.M., Zulfqar, A., Zainab, R., 2020. Naegleria fowleri: sources of infection, pathophysiology, diagnosis, and management; a review. Clin. Exp. Pharmacol. Physiol. 47, 199–212. https://doi.org/10.1111/1440-1681.13192.

Johnson, R.O., Cope, J.R., Moskowitz, M., Kahler, A., Hill, V., Behrendt, K., Molina, L., Fullerton, K.E., Beach, M.J., 2016. Notes from the Field : primary amebic meningoencephalitis associated with exposure to swimming pool water supplied by an overland pipe — inyo county, California, 2015. MMWR Morb. Mortal. Wkly. Rep. 65, 424. https://doi.org/10.15585/mmwr.mm6516a4.

Kaczanowski, S., Sajid, M., Reece, S.E., 2011. Evolution of apoptosis-like programmed cell death in unicellular protozoan parasites. Parasites Vectors 4, 44. https://doi.org/10.1186/1756-3305-4-44.

Laniado-Laborín, R., Cabrales-Vargas, M.N., 2009. Amphotericin B: side effects and toxicity. Rev. Iberoam. De. Micol. https://doi.org/10.1016/j.riam.2009.06.003.

León, A., Del-Ángel, M., Ávila, J.L., Delgado, G., 2017. Phthalides: distribution in nature, chemical reactivity, synthesis, and biological activity. In: Kinghorn, A.D., Falk, H., Gibbons, S., Kobayashi, J. (Eds.), Progress in the Chemistry of Organic Natural Products. Springer International Publishing, Cham, pp. 127–246. https://doi.org/10.1007/978-3-319-45618-8_2.

León, L.G., Ríos-Luci, C., Tejedor, D., Pérez-Roth, E., Montero, J.C., Pandiella, A., García-Tellado, F., Padrón, J.M., 2010. Mitotic arrest induced by a novel family of DNA topoisomerase II inhibitors. J. Med. Chem. 53, 3835–3839. https://doi.org/10.1021/jm100155y.

Liechti, N., Schürch, N., Bruggmann, R., Wittwer, M., 2019. Nanopore sequencing improves the draft genome of the human pathogenic amoeba Naegleria fowleri. Sci. Rep. 9, 16040. https://doi.org/10.1038/s41598-019-52572-0.

Lograd, L.P.L., Santos, C.O., Romeiro, L.A.S., Costa, A.M., Ferreira, J.R.O., Cavalcanti, B.C., Moraes, O.M., Costa-Lotufo, L.V., Pessoa, C., Dos Santos, M.L., 2010. Synthesis and cytotoxicity screening of substituted isobenzofuranones designed from anacardic acids. Eur. J. Med. Chem. 45, 3480–3489. https://doi.org/10.1016/j.ejmech.2010.05.015.

Lopez, C., Budge, P., Chen, J., Bilyeu, S., Mirza, A., Custodio, H., Irazuzta, J., Visvesvara, G., Sullivan, K.J., 2012. Primary amebic meningoencephalitis: a case report and literature review. Pediatr. Emerg. Care 28, 272–276. https://doi.org/10.1097/PEC.0b013e3182495589.

Lorenzo-Morales, J., Díaz-Marrero, A.R., Cen-Pacheco, F., Sifaoui, I., Reyes-Batlle, M., Souto, M.L., Daranas, A.H., Piñero, J.E., Fernández, J.J., 2019. Evaluation of oxasqualenoids from the red Alga laurencia viridis against Acanthamoeba. Mar. Drugs. https://doi.org/10.3390/md17070420.

Lorenzo-Morales, J., Khan, N.A., Walochnik, J., 2015. An update on Acanthamoeba keratitis: diagnosis, pathogenesis and treatment. Parasite 22, 10. https://doi.org/10.1051/parasite/2015010.

Lu, B., Zhao, M., Ding, G., Xie, X., Jiang, L., Ratovelomanana-Vidal, V., Zhang, Z., 2017. Ruthenium-catalyzed enantioselective hydrogenation/lactonization of 2-Acylaryl-carboxylates: direct access to chiral 3-substituted phthalides. ChemCatChem 9, 3989–3996. https://doi.org/10.1002/cctc.201700695.

Maciver, S.K., Piñero, J.E., Lorenzo-Morales, J., 2020. Is naegleria fowleri an emerging parasite? Trends Parasitol. 36, 19–28. https://doi.org/10.1016/j.pt.2019.10.008.

Mal, D., Pahari, P., De, S.R., 2007. Regiospecific synthesis of 3-(2,6-dihydroxyphenyl) phthalides: application to the synthesis of isopestacin and cryphonectric acid. Tetrahedron 63, 11781–11792. https://doi.org/10.1016/j.tet.2007.08.048.

Milanez, G.D., Masangkay, F.R., Thomas, R.C., Ordona, M.O.G.O., Bernales, G.Q., Corpuz, V.C.M., Fortes, H.S.V., Garcia, C.M.S., Nicolas, L.C., Nissapatorn, V., 2017. Molecular identification of Vermamoeba vermiformis from freshwater fish in lake Taal, Philippines. Exp. Parasitol. 183, 201–206. https://doi.org/10.1016/j.exppara.2017.09.009.

Mishra, A., Vinayagam, J., Saha, S., Chowdhury, S., Roychowdhury, S., Jaisankar, P., Majumder, H.K., 2014. Isobenzofuranone derivatives exhibit antileishmanial effect by inhibiting type II DNA topoisomerase and inducing host response. Pharmacol. Res. Perspect. 2, e00070 https://doi.org/10.1002/prp2.70.

Mittal, N., Mahajan, L., Hussain, Z., Gupta, P., Khurana, S., 2019. Primary amoebic meningoencephalitis in an infant. Indian J. Med. Microbiol. 37, 120–122. https://doi.org/10.4103/ijmm.IJMM_18_371.

Mullican, J.C., Chapman, N.M., Tracy, S., 2018. Complete genome sequence of the circular extrachromosomal element of Naegleria gruberi strain EGB ribosomal DNA. Genome Announc. 6 https://doi.org/10.1128/genomeA.00020-18 e00020-18.

Naik, P.K., Santoshi, S., Joshi, H.C., 2012. Noscapinoids with anti-cancer activity against human acute lymphoblastic leukemia cells (CEM): a three dimensional chemical space pharmacophore modeling and electronic feature analysis. J. Mol. Model. 18, 307–318. https://doi.org/10.1007/s00894-011-1057-9.

Pereira, W.L., De Souza Vasconcellos, R., Mariotini-Moura, C., Gomes, R.S., De Cássia Firmino, R., Da Silva, A.M., Júnior, A.S., Bressan, G.C., Almeida, M.R., Afonso, L.C. C., Teixeira, R.R., Fietto, J.L.R., McPhee, D.J., 2015. The antileishmanial potential of C-3 functionalized isobenzofuranones against Leishmania (Leishmania) Infantum Chagasi. Molecules. https://doi.org/10.3390/molecules201219857.

Phan, D.H.T., Kim, B., Dong, V.M., 2009. Phthalides by rhodium-catalyzed ketone hydroacylation. J. Am. Chem. Soc. 131, 15608–15609. https://doi.org/10.1021/ja907711a.

Piñero, J.E., Chávez-Munguía, B., Omaña-Molina, M., Lorenzo-Morales, J., 2019. Naegleria fowleri. Trends Parasitol. 35, 848–849. https://doi.org/10.1016/j.pt.2019.06.011.

Rahman, M.M., Lopa, S.S., Sadik, G., Harun-Or-Rashid, Islam, R., Khondkar, P., Alam, A. H.M.K., Rashid, M.A., 2005. Antibacterial and cytotoxic compounds from the bark of Cananga odorata. Fitoterapia 76, 758–761. https://doi.org/10.1016/j.fitote.2005.08.011.

Rice, C.A., Colon, B.L., Alp, M., Göker, H., Boykin, D.W., Kyle, D.E., 2015. Bis-benzimidazole hits against Naegleria fowleri discovered with new high-throughput screens. Antimicrob. Agents Chemother. 59, 2037–2044. https://doi.org/10.1128/AAC.05122-14.

Rizo-Liendo, A., Arberas-Jiménez, I., Sifaoui, I., Reyes-Batlle, M., Piñero, J.E., Lorenzo-Morales, J., 2021. The type 2 statins, cerivastatin, rosuvastatin and pitavastatin eliminate Naegleria fowleri at low concentrations and by induction of programmed cell death (PCD). Bioorg. Chem. 110, 104784. https://doi.org/10.1016/j.bioorg.2021.104784.

Rizo-Liendo, Aitor, Sifaoui, I., Arberas-Jiménez, I., Reyes-Batlle, M., Piñero, J.E., Lorenzo-Morales, J., 2020a. Fluvastatin and atorvastatin induce programmed cell death in the brain eating amoeba Naegleria fowleri. Biomed. Pharmacother. 130 https://doi.org/10.1016/j.biopha.2020.110583.

Rizo-Liendo, Aitor, Sifaoui, I., Cartuche, L., Arberas-Jiménez, I., Reyes-Batlle, M., Fernández, J.J., Piñero, J.E., Díaz-Marrero, A.R., Lorenzo-Morales, J., 2020b. Evaluation of indolocarbazoles from streptomyces sanyensis as a novel source of therapeutic agents against the brain-eating amoeba naegleria fowleri. Microorganisms 8, 789. https://doi.org/10.3390/microorganisms8050789.

Rizo-Liendo, A., Sifaoui, I., Cartuche, L., Arberas-Jiménez, I., Reyes-Batlle, M., Fernández, J.J., Piñero, J.E., Díaz-Marrero, A.R., Lorenzo-Morales, J., 2020. Evaluation of indolocarbazoles from streptomyces sanyensis as a novel source of therapeutic agents against the brain-eating amoeba naegleria fowleri. Microorganisms 8. https://doi.org/10.3390/microorganisms8050789.

Rizo-Liendo, A., Sifaoui, I., Reyes-Batlle, M., Chiboub, O., Rodríguez-Expósito, R.L., Bethencourt-Estrella, C.J., Nicolás-Hernández, D.S., Hendiger, E.B., López-Arencibia, A., Rocha-Cabrera, P., Piñero, J.E., Lorenzo-Morales, J., 2019. In vitro activity of statins against Naegleria fowleri. Pathogens. https://doi.org/10.3390/pathogens8030122.

Sánchez-Fernández, R.E., Sánchez-Fuentes, R., Rangel-Sánchez, H., Hernández-Ortega, S., López-Cortés, J.G., Macías-Rubalcava, M.L., 2020. Antifungal and antioomycete activities and modes of action of isobenzofuranones isolated from the endophytic fungus Hypoxylon anthochroum strain Gseg1. Pestic. Biochem. Physiol. 169, 104670. https://doi.org/10.1016/j.pestbp.2020.104670.

Siddiqui, R., Ali, I.K.M., Cope, J.R., Khan, N.A., 2016. Biology and pathogenesis of Naegleria fowleri. Acta Trop. 164, 375–394. https://doi.org/10.1016/j.actatropica.2016.09.009.

Sifaoui, I., López-Arencibia, A., Martín-Navarro, C.M., Reyes-Batlle, M., Mejri, M., Valladares, B., Lorenzo-Morales, J., Abderabba, M., Piñero, J.E., 2017. Selective activity of oleanolic and maslinic acids on the amastigote form of Leishmania spp. Iran. J. Pharm. Res. 16, 1192–1195. https://doi.org/10.22037/ijpr.2017.2070.

Sifaoui, I., Reyes-Batlle, M., López-Arencibia, A., Chiboub, O., Rodríguez-Martín, J., Rocha-Cabrera, P., Valladares, B., Piñero, J.E., Lorenzo-Morales, J., 2018. Toxic effects of selected proprietary dry eye drops on Acanthamoeba. Sci. Rep. 8, 8520. https://doi.org/10.1038/s41598-018-26914-3.

Strobel, G., Ford, E., Worapong, J., Harper, J.K., Arif, A.M., Grant, D.M., Fung, P.C.W., Ming Wah Chau, R., 2002. Isopestacin, an isobenzofuranone from Pestalotiopsis

microspora, possessing antifungal and antioxidant activities. Phytochemistry 60, 179–183. https://doi.org/10.1016/S0031-9422(02)00062-6.

Teixeira, R.R., Bressan, G.C., Pereira, W.L., Joana Gasperazzo, Ferreira, De Oliveira, F. M., Thomaz, D.C., 2013. Synthesis and antiproliferative activity of C-3 functionalized isobenzofuran-1(3H)-ones. Molecules. https://doi.org/10.3390/molecules18021881.

Tejedor, D., Cotos, L., Márquez-Arce, D., Odriozola-Gimeno, M., Torrent-Sucarrat, M., Cossío, F.P., García-Tellado, F., 2015. Microwave-assisted organocatalyzed rearrangement of propargyl vinyl ethers to salicylaldehyde derivatives: an experimental and theoretical study. Chem. Eur J. 21, 18280–18289. https://doi.org/10.1002/chem.201503171.

Tejedor, D., García-Tellado, F., Marrero-Tellado, J.J., De Armas, P., 2003. Efficient domino process based on the catalytic generation of non-metalated, conjugated acetylides in the presence of aldehydes or activated ketones. Chem. Eur J. 9, 3122–3131. https://doi.org/10.1002/chem.200204579.

Tejedor, D., López-Tosco, S., Méndez-Abt, G., Cotos, L., García-Tellado, F., 2016. Propargyl vinyl ethers and tertiary skipped diynes: two pluripotent molecular platforms for diversity-oriented synthesis. Acc. Chem. Res. 49, 703–713. https://doi.org/10.1021/acs.accounts.5b00545.

Tejedor, D., Méndez-Abt, G., Cotos, L., Ramirez, M.A., García-Tellado, F., 2011. A microwave-assisted domino rearrangement of propargyl vinyl ethers to multifunctionalized aromatic platforms. Chem. Eur J. 17, 3318–3321. https://doi.org/10.1002/chem.201003532.

Tian, X., Li, H.-M., Wei, J.-Y., Liu, B.-J., Zhang, Y.-H., Wang, G.-J., Chang, J.-B., Qiao, H.-L., 2016. Preclinical pharmacokinetics, tissue distribution, and plasma protein binding of Sodium (±)-5-Bromo-2-(α-Hydroxypentyl) benzoate (BZP), an innovative potent anti-ischemic stroke agent. Front. Pharmacol. https://doi.org/10.3389/fphar.2016.00255.

Tillery, L., Barrett, K., Goldstein, J., Lassner, J.W., Osterhout, B., Tran, N.L., Xu, L., Young, R.M., Craig, J., Chun, I., Dranow, D.M., Abendroth, J., Delker, S.L., Davies, D. R., Mayclin, S.J., Calhoun, B., Bolejack, M.J., Staker, B., Subramanian, S., Phan, I., Lorimer, D.D., Peter, J.M., Edwards, T.E., Kyle, D.E., Rice, C.A., Morris, J.C., Leahy, J.W., Manetsch, R., Barrett, L.K., Smith, C.L., Van Voorhis, W.C., 2021. Naegleria fowleri: protein structures to facilitate drug discovery for the deadly, pathogenic free-living amoeba. PLoS One 16 (3). https://doi.org/10.1371/journal.pone.0241738.

Touchet, S., Kommidi, S.S.R., Gros, P.C., 2018. Organomagnesiate-promoted enantioselective cascade process: straightforward access to chiral 3-substituted isobenzofuranones. Chemistry 3, 3939–3942. https://doi.org/10.1002/slct.201800178.

Trabelsi, H., Dendana, F., Sellami, A., Sellami, H., Cheikhrouhou, F., Neji, S., Makni, F., Ayadi, A., 2012. Pathogenic free-living amoebae: epidemiology and clinical review. Pathol. Biol. 60, 399–405. https://doi.org/10.1016/j.patbio.2012.03.002.

Visvesvara, G.S., Moura, H., Schuster, F.L., 2007. Pathogenic and opportunistic free-living amoebae: Acanthamoeba spp., Balamuthia mandrillaris, Naegleria fowleri, and Sappinia diploidea. FEMS Immunol. Med. Microbiol. 50, 1–26. https://doi.org/10.1111/j.1574-695X.2007.00232.x.

Xing, C.H., Liao, Y.X., He, P., Hu, Q.S., 2010. Transition metal-catalyzed addition reactions of arylboronic acids with alkyl 2-formylbenzoates: efficient access to chiral 3-substituted phthalides. Chem. Commun. 46, 3010–3012. https://doi.org/10.1039/c001104e.

Yang, J., Yoshikai, N., 2014. Cobalt-catalyzed enantioselective intramolecular hydroacylation of ketones and olefins. J. Am. Chem. Soc. 136, 16748–16751. https://doi.org/10.1021/ja509919x.

Yoder, J.S., Eddy, B.A., Visvesvara, G.S., Capewell, L., Beach, M.J., 2010. The epidemiology of primary amoebic meningoencephalitis in the USA, 1962-2008. Epidemiol. Infect. 138, 968–975. https://doi.org/10.1017/S0950268809991014.

Yoder, J.S., Straif-Bourgeois, S., Roy, S.L., Moore, T.A., Visvesvara, G.S., Ratard, R.C., Hill, V.R., Wilson, J.D., Linscott, A.J., Crager, R., Kozak, N.A., Sriram, R., Narayanan, J., Mull, B., Kahler, A.M., Schneeberger, C., Da Silva, A.J., Poudel, M., Baumgarten, K.L., Xiao, L., Beach, M.J., 2012. Primary amebic meningoencephalitis deaths associated with sinus irrigation using contaminated tap water. Clin. Infect. Dis. 55, e79–e85. https://doi.org/10.1093/cid/cis626.

Yohda, M., Yamamoto, Y., 2015. Enantioselective addition of arylboronic acids to methyl 2-formylbenzoates by using a ruthenium/Me-BIPAM catalyst for synthesis of chiral 3-aryl-isobenzofuranones. Org. Biomol. Chem. 13, 10874–10880. https://doi.org/10.1039/c5ob01661d.

Zeouk, I., Sifaoui, I., Rizo-Liendo, A., Arberas-Jiménez, I., Reyes-Batlle, M., Bazzocchi, I., Bekhti, K., Piñero, J., Jiménez, I.A., Lorenzo-Morales, J., 2021. Exploring the anti-infective value of inuloxin A isolated from inula viscosa against the brain-eating amoeba (naegleria fowleri) by activation of programmed cell death. ACS Chem. Neurosci. 12, 195–202. https://doi.org/10.1021/acschemneuro.0c00685.

Zeouk, I., Sifaoui, I., Rizo-Liendo, A., Arberas-Jiménez, I., Reyes-Batlle, M., Bazzocchi, I. L., Bekhti, K., Piñero, E., Jiménez, I.A., Lorenzo-Morales, J., 2020. Exploring the anti-infective value of inuloxin A isolated from inula viscosa against the brain-eating amoeba (naegleria fowleri) by activation of programmed cell death. ACS Chem. Neurosci. https://doi.org/10.1021/acschemneuro.0c00685.